View metadata, citation and similar papers at core.ac.uk

brought to you by CORE

provided by Elsevier - Publisher Connector

International Journal of Solids and Structures 47 (2010) 2201–2214

Contents lists available at ScienceDirect

International Journal of Solids and Structures

journal homepage: www.elsevier.com/locate/ijsolstr

Effects of the pH on the mechanical behavior of articular cartilage and corneal stroma

Benjamin Loret [a,*], Fernando M.F. Simões [b]

[a] Laboratoire Sols, Solides, Structures, B.P. 53X, 38041 Grenoble Cedex, France
[b] ICIST and Departamento de Engenharia Civil, Instituto Superior Técnico, TU Lisbon, Av. Rovisco Pais, 1049-001 Lisboa, Portugal

ARTICLE INFO

Article history:
Received 11 September 2009
Received in revised form 22 March 2010
Available online 24 April 2010

Keywords:
Electro-chemo-mechanical couplings
Acid–base reactions
Fixed electric charge
Soft tissues
Ion binding

ABSTRACT

Electro-chemo-mechanical couplings in articular cartilages and corneal stroma are due to the presence of electric charges on proteoglycans. In addition, at non-physiological pH, collagen molecules become charged as well. Variation of the pH of the electrolyte has strong implications on the electric charge of these tissues, and by the same token, on their transport and mechanical properties. Indeed, articular cartilages and corneal stroma swell and shrink depending on the composition of the electrolyte, they are in contact with.

Emphasis is laid here on the combined effects of pH, ionic strength, calcium and chloride binding on mechanical properties.

The tissues are viewed as three-phase multi-species porous media. The constitutive framework is phrased in the theory of thermodynamics of deformable porous media. Acid–base reactions, as well as ion binding, are embedded in this framework. Although, macroscopic in nature, the approach accounts for a number of biochemical details defining collagen and proteoglycans.

The model is used to simulate laboratory experiments where specimens of articular cartilages and corneal stroma are put in contact with a bath of controlled chemical composition. Chemical loadings, where the ionic composition and pH of the bath are varied, are intermingled with mechanical loadings. The variations of the stress and strain are observed to depend strongly on the ionic strength and ion type present in the bath: sodium chloride leads to a stiffer response than calcium chloride and hydrochloric acid. Moreover, when the bath changes from basic to acidic, the change of sign of the fixed charge across the isoelectric point has definite mechanical implications, and it gives rise to non-monotonous evolutions of the stress, strain and chemical content.

While the *chemo-mechanical effect* is a key phenomenon that governs the behavior of tissues with fixed charges, the converse *mechano-chemical effect* is significant in corneal stroma due to its low stiffness.

© 2010 Elsevier Ltd. All rights reserved.

1. Introduction

Articular cartilages and corneal stroma are porous media, structured by collagen fibrils, and saturated by an electrolyte, where metallic ions are bathed in water. Roughly speaking, under constant load, these tissues swell if the ionic strength of the bath they are in contact with decreases, and conversely they shrink if the ionic strength increases. On the other hand, at given strain, the equilibrium stress increases as the ionic strength decreases (Eisenberg and Grodzinsky, 1985). Charged macromolecules, the proteoglycans (PG's), intermingled with collagen fibrils, give rise to electro-chemo-mechanical couplings that allow moderate deformation to take place, and ensure an optimal adaption of the tissues to physiological loads.

The collagen that structures articular cartilages is mainly of type II. Its amino acids contain, linked to a central carbon, a hydrogen atom, a side chain, an amino group NH_3^+, and a carboxyl group COO^-, often referred to as N- and C-terminus, respectively. The N- and C-termini of two successive amino acids engage in rather stable peptide bonds. Some of the side chains are electrically charged. The charges essentially balance at neutral pH. On the other hand, due to the amino- and carboxyl groups of these side chains, the collagen molecule becomes positively charged at low pH, and negatively charged at high pH.

Proteoglycans aggregate along a hyaluronate protein, to which 40 to 60 subunits are attached through a specific link protein. The subunit, referred to as proteoglycan molecule (PG), is constituted by a number of glycosaminoglycans (GAG's), which are attached along a core protein. GAG's are formed by disaccharide

* Corresponding author. Tel.: +33 476 825298; fax: +33 476 827000.
E-mail addresses: Benjamin.Loret@inpg.fr, benjamin.loret@hmg.inpg.fr (B. Loret), fsimoes@civil.ist.utl.pt (F.M.F. Simões).

0020-7683/$ - see front matter © 2010 Elsevier Ltd. All rights reserved.
doi:10.1016/j.ijsolstr.2010.04.010

units, with one uronic acid containing a carboxyl COO^-, and a variable number of amino sugars containing a sulfate SO_3^-.

The two main types of GAG's in articular cartilages are chondroitin sulfates (CS) and keratan sulfates (KS). Keratan sulfates are shorter than chondroitin sulfates, and contain about half the number of disaccharide units (Muir, 1978). They possess no uronic acid (carboxyl group), so that their charge is -1, while chondroitin sulfates have a charge equal to -2.

The charge of the two main non-soluble components of articular cartilages and corneal stroma, namely collagen and proteoglycans, is said to be *fixed*, in contrast to that of *mobile* ions, typically sodium Na^+, calcium Ca^{2+} and chloride Cl^-. The presence of the hydrogen ion H^+ and hydroxyl ion OH^-, in addition to metallic ions, strongly affects the transport and mechanical properties. This is due to the fact that the fixed electric charge varies with pH.

Corneal stroma presents some qualitative similarities with articular cartilages. While the fixed charge is due to PG's at neutral pH, collagen contributes at low and high pHs, similar to articular cartilages. However, the actual composition, magnitude of the fixed charge and structure of these tissues reflect the fact that their biological functions are quite distinct. Even if chondroitin sulfates and keratan sulfates are the main GAG's of both articular cartilages and stroma, the number of disaccharide units they display are quite different. Unlike articular cartilages which are composed of type II collagen, corneal stroma displays mainly type I collagen.

In the corneal stroma, the collagen fibrils form essentially a planar network. They are embedded in lamellae and oriented parallel to the corneal surface. At each point, they are grouped along two main directions that are orthogonal in the center of the cornea but become circumferential at the limbus. Thus swelling takes place essentially along the radial direction.

As for articular cartilages, the concentration and directional distribution of collagen vary across the thickness of the cartilage layer. Collagen fibrils are oriented parallel to the joint in the upper zone, orthogonal to the subchondral bone in the lower zone, and their directional distribution is approximately random in the central zone.

Chloride binding on ligands of unknown composition but associated with collagen fibrils contributes to the fixed charge of the stroma. On the other hand, calcium binding is usually neglected in standard analyses of articular cartilage. However, the simulations of laboratory experiments that include high concentrations of calcium chloride, as those studied here, require that phenomenon to be accounted for.

The most fundamental characteristic of cornea is the presence of ionic pumps located mainly over its endothelium that are thought to limit swelling, and ensure transparency. However, since the stromal specimens we consider are de-epithelized, we can dispense with the active transport issue, and concentrate on the interactions between pH and mechanics.

1.1. Quantitative data

The presence of a fixed electric charge is a key element of the mechanical and transport properties of articular cartilages and stroma. This charge is modified by acid–base reactions (binding-release of hydrogen ions), and reversible or irreversible binding of some metallic ions.

A clear distinction should be made between the pH of the bath, the tissue is in contact with, and the pH of the electrolyte that circulates the tissue. Indeed, the presence of the electric charge implies a number of mechanical properties (pressure, etc.), electrical properties (electrical potential), and chemical properties (concentrations), to be discontinuous at the bath/tissue interface. Still, the tissue pH, say extrafibrillar pH, can be modified by a variation of the pH of the bath, as well as by a variation of its ionic strength.

A number of experimental observations guide the development of the model of the chemo-mechanical couplings to be presented below:

- The aggregate isoelectric point (IEP) corresponds to the balance between the negatively charged carboxyl groups COO^- and sulfate groups SO_3^- and the amino groups NH_3^+. The isoelectric point for bovine articular cartilages has been reported in the range of pH from about 2.5 to 3 (Frank and Grodzinsky, 1987, p. 626). The IEP displayed in the experiments on bovine corneal stroma by Huang and Meek (1999) is slightly higher, about 4. Note that, while the pHs of the bath and tissue are in general different, they are equal just at the IEP. A macroscopic manifestation of the modification of the fixed charge, actually its change of sign, is the reversal of the electro-osmotic flow. Actually, the sign of the electro-osmotic coefficient is opposite to that of the fixed electric charge. Thus, while electro-osmosis implies water to move towards the cathode above the isoelectric point, reversal of the electro-osmotic flow takes place at very low pH below the isoelectric point.
- Another manifestation of the change of the magnitude and sign of the fixed charge is of mechanical nature. In a uniaxial traction test at given axial strain, but varying pH, the equilibrium stress shows a minimum at the IEP (Grodzinsky et al., 1981, Fig. 8). Increase of HCl concentration (in bath) from pH 7 to 2.6 is accompanied with a decrease of the equilibrium stress. However, as the pH decreases further, the stress undergoes a rebound. Indeed, the cartilage charge becomes positive below the isoelectric point. The stress is expected to vary in proportion with the absolute value of the fixed charge, since the latter, whatever its sign, triggers repulsion between cartilage units.
  In a much similar vein, while testing bovine corneal stroma isotropically compressed via polyethylene glycol, Huang and Meek (1999) observe that the relative hydration, namely ratio of wet weight over dry weight, shows a minimum at the isoelectric point, and undergoes a drastic rebound below the IEP.
- The repulsion between charged units is shielded by mobile ions: the higher the ionic strength, the smaller the actual repulsion. In other words, at large ionic strength, electrical shielding overweighs essentially, if not completely, the electro-chemo-mechanical couplings induced by the fixed charge. According to Grodzinsky et al. (1981), increasing ionic strength in presence of NaCl and $CaCl_2$ decreases the equilibrium stress of cartilages, but in a monotonic way. $CaCl_2$ is more efficient to decrease the equilibrium stress than NaCl. Still, it has been conjectured in Loret and Simões (2005a,b) that the hypertonic state (at large concentrations) is unique, and independent of the shielding ions.

The only model that addresses the influence of pH on the transport properties of articular cartilages has been exposed by Frank et al. (1990). Besides considering both binary and ternary electrolytes with ion binding, Loret and Simões (2010) have restated the problem within the theory of mixtures.

1.2. Scope

In a further effort along the same perspective of the theory of mixtures, emphasis is laid here on the effects of pH on the mechanical properties.

The theoretical framework draws upon earlier work (Loret and Simões, 2004, 2005a,b, 2007), and will be briefly sketched in Section 2. Details of the biochemical composition of the collagen, proteoglycans and glycosaminoglycans are essential ingredients of this model, which although macroscopic in nature, takes account of a number of biochemical properties, Section 2.3.

Incorporation of the acid–base reactions and of calcium or chloride binding into the thermodynamical construction is a main contribution of this work. It is performed in Section 3.

Since the data that will be simulated involve uniaxial traction, the model applied to confined compression in Loret and Simões (2004, 2005a,b) needs to be modified. The purely mechanical response is contributed by an isotropic matrix (ground substance) and by the collagen network. A directional model is developed that includes some nonlinear effects due to the fact that the directions along which fibers are mechanically active depend on both the mechanical and chemical loadings, Section 4. Swelling is observed to induce stiffening of the purely mechanical behavior of the cartilage. Conversely, lateral shrinking leads to mechanical softening.

The general framework introduced in Section 3 is particularized in Section 4.3, where a prototype of chemo-mechanical model including the influence of ionic strength and pH on the mechanical response (stress, strain) is developed.

In actual laboratory experiments, a cartilage specimen is bathed in a reservoir of controlled chemical composition and controlled mechanical conditions. The ensuing chemical composition of the cartilage at equilibrium can be obtained as sketched in Section 3.5. Laboratory experiments in which either the ionic strength, or the pH of the bath, are varied can then be mimicked by the model, Section 5. The simulations are compared with experimental data obtained from bovine femoropatellar joints taken from animals of 1 to 2 year old (Grodzinsky et al., 1981).

While the bulk of the developments below addresses primarily articular cartilages, simulations of experiments on bovine corneal stroma by Huang and Meek (1999) will serve to highlight similarities and qualitative differences between articular cartilages and corneal stroma.

To simplify the analysis, all the species themselves that constitute the tissues are considered to be incompressible.

Notation: Vector and tensor quantities are identified by boldface letters. Symbols '·' and ':' between tensors of various orders denote their inner product with single and double contraction, respectively. tr denotes the trace of a second order tensor, and $\mathbf{I}$ the second order identity tensor. Unless stated otherwise, the convention of summation over repeated indices does not apply.

2. The mixture framework

2.1. The constituents and phases

Articular cartilage is viewed as a three-phase, multi-species, porous medium. The *solid phase S* is constituted by collagen fibrils denoted by the symbol c. Proteoglycans PG's are considered to be bathed in the *extrafibrillar fluid phase* E. The latter contains water w, sodium ions Na^+, and/or calcium ions Ca^{2+}, chloride ions Cl^-, hydrogen ions H^+ and hydroxyl ions OH^-,

$$\mathrm{S} = \{\mathrm{c}\}, \quad \mathrm{E} = \{\mathrm{w}, \mathrm{PG}, \mathrm{Na}, \mathrm{Ca}, \mathrm{Cl}, \mathrm{H}, \mathrm{OH}\}. \tag{2.1}$$

The *intrafibrillar fluid phase* contains the same species as the *extrafibrillar fluid phase* but proteoglycans PG's. Species of the intrafibrillar fluid phase have no access to the surrounding, and must be first transferred to the extrafibrillar phase. Only the extrafibrillar phase communicates with the surroundings. Motivation for the phase segregation and hierarchical structure adopted is presented in Loret and Simões (2004).

Water and ions in the extrafibrillar phase are endowed with their own velocities so as to allow water to flow through the solid skeleton and ions to diffuse in this phase and satisfy their own balance of momentum. On the other hand, the proteoglycans move with the solid phase.

For pH close to 7, collagen can be considered electrically neutral (Li and Katz, 1976). However, at non-physiological pH, collagen becomes charged. Topological considerations seem to indicate that electroneutrality should be ensured separately for the two fluid compartments. Since collagen is in contact with both compartments, a partition of the charge should be defined.

2.2. Macroscopic descriptors of the geometry and mass of the mixture

Various macroscopic measures of mass and volume are used to formulate the constitutive equations. They are defined below.

Let the initial volume of the porous medium be V_0 and let $V = V(t)$ be its current volume. The current mole number, volume and mass of the species l of phase K are denoted by $N_{l\mathrm{K}}$, $V_{l\mathrm{K}}$ and $M_{l\mathrm{K}}$, respectively. Various additional entities are attached to species:

- Some are intrinsic like the intrinsic density ρ_l, the molar volume $\hat{v}_l$ and molar mass $\hat{m}_l$ linked by $\hat{m}_l = \rho_l \hat{v}_l$.
- Some refer to the current volume, like the *volume fraction* $n^{l\mathrm{K}} = V_{l\mathrm{K}}/V$.
- Some refer to the initial volume like the *mole content* $\mathcal{N}_{l\mathrm{K}} = N_{l\mathrm{K}}/V_0$, the *volume content* $v^{l\mathrm{K}} = V_{l\mathrm{K}}/V_0 = n^{l\mathrm{K}} V/V_0$, the *mass content* $m^{l\mathrm{K}} = M_{l\mathrm{K}}/V_0 = \rho_l v^{l\mathrm{K}}$.

The corresponding entities associated with the phase K are defined by algebraic summation of individual contributions, e.g. the current volume V_K and mass M_K, the volume fraction $n^\mathrm{K} = V_\mathrm{K}/V$. Volume fractions satisfy the compatibility relation $\sum_\mathrm{K} n^\mathrm{K} = 1$.

Other entities live in their phase, e.g. the molar fractions and the concentrations. The *molar fraction* $x_{l\mathrm{K}}$ of the species l in phase K is defined by the ratio of the mole number $N_{l\mathrm{K}}$ of that species over the total number N_K of moles within the phase, $x_{l\mathrm{K}} = N_{l\mathrm{K}}/N_K$. In each phase, the molar fractions satisfy the compatibility relation $\sum_{l\in\mathrm{K}} x_{l\mathrm{K}} = 1$. Since $N_{l\mathrm{K}}/V_0 = m^{l\mathrm{K}}/\hat{m}_l$, the molar fractions can also be expressed in terms of mass contents.

The *concentration* of an extrafibrillar species is equal to its number of moles referred to the volume of extrafibrillar phase,

$$c_{l\mathrm{E}} = \frac{N_{l\mathrm{E}}}{V_\mathrm{E}} = \frac{x_{l\mathrm{E}}}{\hat{v}_\mathrm{E}}, \quad l \in \mathrm{E}, \tag{2.2}$$

with $\hat{v}_\mathrm{E} = \sum_{l\in\mathrm{E}} x_{l\mathrm{E}} \hat{v}_l \simeq \hat{v}_\mathrm{w}$ the molar volume of the extrafibrillar fluid phase.

Collagen and proteoglycans are macromolecules with a large molar mass, 0.285×10^6 g for collagen and 2×10^6 g for PG's. The molar fraction $x_l = N_l/N_\mathrm{E}$ and concentration $c_l = N_l/V_\mathrm{E}$ of proteoglycans ($l = \mathrm{PG}$) and collagen ($l = \mathrm{c}$) are thus quite small with respect to the other species of the extrafibrillar phase. On the other hand, the valence ζ_PG of proteoglycans is large at neutral pH, while the valence ζ_c of collagen is large at non-physiological pH. The *effective* molar fraction y_l and *effective* concentration e_l,

$$\underbrace{y_l = \zeta_l x_l}_{\text{effective molar fraction}}, \qquad \underbrace{e_l = \zeta_l c_l}_{\text{effective concentration}}, \qquad l = \mathrm{PG}, \mathrm{c}, \tag{2.3}$$

are key parameters of the biochemical and biomechanical behaviors of cartilages.

The total effective molar fraction y_e and concentration e_e of the extrafibrillar charge including PG's and collagen are similarly defined in terms of valences and mole numbers,

$$y_\mathrm{e} = \zeta_\mathrm{PG} \frac{N_\mathrm{PG}}{N_\mathrm{E}} + \zeta_\mathrm{c} \frac{N_\mathrm{c}}{N_\mathrm{E}}, \quad e_\mathrm{e} = \zeta_\mathrm{PG} \frac{N_\mathrm{PG}}{V_\mathrm{E}} + \zeta_\mathrm{c} \frac{N_\mathrm{c}}{V_\mathrm{E}}, \tag{2.4}$$

and then $y_\mathrm{e} = e_\mathrm{e} \hat{v}_\mathrm{E} \sim e_\mathrm{e} \hat{v}_\mathrm{w}$.

Incidentally, it should be realized, that the change of volume of the porous medium modifies the concentrations of species, since

the volume of the fluid phase is affected. The ensuing analytical relations are easily established.

2.3. The contributions to the extrafibrillar fixed charge

A number of data defining the species (PG's, collagen, water) that compose the cartilage as well as their proportions is required. Some key details on the origin of the fixed electric charge are provided below.

2.3.1. Composition of GAG's

Glycosaminoglycans (GAG's) contain $N_{\rm du}^{\rm CS}=25$ moles of disaccharide units per mole of chondroitin sulfate, and the number $N_{\rm CS}$ of moles of chondroitin sulfate in a mole of PG's is about 80. The corresponding numbers for keratan sulfates are 13 and 40, respectively. From these data, the numbers of moles of carboxyl groups $N_{\rm cg}^{\rm PG}$ and of sulfate groups $N_{\rm sg}^{\rm PG}$ in $N_{\rm PG}$ moles of PG's, and the valence $\zeta_{\rm PG}$ of PG's can be deduced:

$$\zeta_{\rm PG}=(-2)N_{\rm du}^{\rm CS}\times\frac{N_{\rm CS}}{N_{\rm PG}}+(-1)N_{\rm du}^{\rm KS}\times\frac{N_{\rm KS}}{N_{\rm PG}}=-4520. \tag{2.5}$$

The above data are extracted from Muir (1978, pp. 68–69) and Muir (1983, p. 613).

2.3.2. Composition and partition of collagen

$N_{\rm c}$ moles of mature collagen of type II contain $N_{\rm ag}^{(\rm c)}=273N_{\rm c}$ moles of charged amino groups, and $N_{\rm cg}^{(\rm c)}=264N_{\rm c}$ moles of charged carboxyl groups (Wachtel and Maroudas, 1998).

The diffusive properties of cartilage are thought to be linked mainly to the extrafibrillar water. Intrafibrillar water is considered to be part of another phase. To account for this water partition, the carboxyl and amino sites of collagen are partitioned as well. About two third of them contribute to the extrafibrillar phase, and one third to the intrafibrillar phase. This proportion has been adopted so as to obtain an isoelectric point (IEP) in the range indicated by Frank and Grodzinsky (1987), namely IEP about 2.6.

2.3.3. The pH profile of the extrafibrillar fixed charge

The pH of the bath ($\rm pH_B$) and of the (extrafibrillar) water circulating the cartilage ($\rm pH_E$) are different, since the chemical compositions are not identical, due to the presence of the fixed charge in the cartilage. The issue of defining $\rm pH_E$ from the chemical composition of the bath, the cartilage is in equilibrium with, will be addressed in the next sections.

In a first step, it is worth displaying the variations of the charge of PG's and collagen as a function of the pH of the extrafibrillar fluid, Fig. 1. These variations arise due to acid–base reactions at specific sites of PG's and collagen, as explained in detail in Section 3. From pH 4 to 8, the charges of both PG's and collagen are practically constant: collagen is about neutral, while PG's are negatively charged. At higher pH, the amino sites of collagen turn from positively charged to neutral. At low pH, the carboxyl sites of both PG's and collagen become neutral. Altogether, PG's are always negatively charged, while the charge of collagen is positive at pH < 4 and negative at pH > 8. The aggregate isoelectric point ranges from about 2.5 to 3.5.

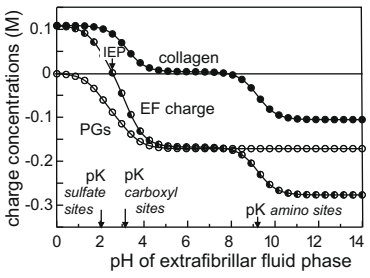

Fig. 1. Contributions of PG's, collagen to the extrafibrillar charge of cartilage as a function of the pH of the fluid of the cartilage, for a constant volume fraction of extrafibrillar fluid $n^{\rm E}=0.8$. From Loret and Simões (2010).

The additional effect of calcium binding to the carboxyl sites of PG's onto the electric charge will be considered in the next section.

3. Constitutive framework including pH effects

Cartilage, with a solid skeleton constituted by proteoglycans, collagen and non-collagenous proteins, is a porous medium circulated by a fluid phase in which sodium and calcium ions and chloride anions diffuse. Ions hydrogen and hydroxyl are present due to water dissociation, and possible chemical loadings. The intrafibrillar fluid and the associated collagen sites do not come into consideration in this approach. The extrafibrillar species and the associated collagen sites satisfy an electroneutrality condition, and they undergo the same electrical field.

The acid–base reactions are considered to be reversible. There are macroscopic arguments that sustain this point of view. For example, in a traction test at given axial strain, subsequent to acidification through hydrochloric acid HCl, Grodzinsky et al. (1981) increase the concentration of sodium hydroxide NaOH: they observe that the stress–pH curve does not show hysteresis.

3.1. Electro-chemical potentials

The incremental works done per unit initial volume V_0 by the stress $\mathbf{T}$ in the incremental strain $\delta\mathbf{E}$ and by the *electro-chemical potentials* $g_{l\rm K}^{\rm ec}$ during the addition/subtraction of the mole contents $\delta\mathscr{N}_{l\rm K}$ of the species l to the phase K sum to

$$\delta\mathscr{W}=\mathbf{T}:\delta\mathbf{E}+\sum_{l\in\rm K}g_{l\rm K}^{\rm ec}\delta\mathscr{N}_{l\rm K}. \tag{3.1}$$

Here, $(\mathbf{T},\mathbf{E})$ is a work-conjugated stress–strain pair. With $\mathbf{F}$ the deformation gradient, $\mathbf{E}$ is typically the Green strain $\frac{1}{2}(\mathbf{F}^{\rm T}\cdot\mathbf{F}-\mathbf{I})$, and $\mathbf{T}$ the second Piola–Kirchhoff stress with respect to the reference configuration linked to the Cauchy stress $\boldsymbol{\sigma}$ by the relation $\mathbf{T}=\det\mathbf{F}\,\mathbf{F}^{-1}\cdot\boldsymbol{\sigma}\cdot\mathbf{F}^{-\rm T}$. The electro-chemical potentials $g_{l\rm K}^{\rm ec}$ (unit: kg/mol × $\rm m^2/s^2$) are mole-based while the mole contents per unit initial volume of the porous medium $\mathscr{N}_{l\rm K}$'s are measured in mole/$\rm m^3$.

The chemical potential $g_{l\rm K}$ of a species l identifies a pressure contribution introduced by the intrinsic pressure $p_{l\rm K}$ and the molar volume $\hat{v}_l$ and a chemical contribution which accounts for the molar fraction $x_{l\rm K}$. For a charged species in presence of the electrical potential $\phi_{\rm K}$ (unit: V), the electro-chemical potential involves in addition an electrical contribution. For incompressible species,

$$g_{l\rm K}^{\rm ec}=\hat{v}_l p_{l\rm K}+RT\ln x_{l\rm K}+\zeta_l{\rm F}\phi_{\rm K},\quad l\in{\rm K}. \tag{3.2}$$

In this formula, $R=8.31451$ J/mol/K is the universal gas constant, T (K) the absolute temperature, and F = 96,485 C/mol is Faraday's equivalent charge (1 C = 1 A × s). The ζ's are the valences. In the extrafibrillar phase, chemo-mechanical couplings imply ions and water to be endowed with their own intrinsic pressure $p_{l\rm E}$. The enthalpy of formation up to the reference configuration, which generates an equilibrium constant different from one, is assumed to be contained in $p_{l\rm E}$ (Loret and Simões, 2005a,b).

3.2. Acid–base reactions and calcium binding

The sites for acid–base reactions and calcium binding which are accounted for in this analysis are displayed in Fig. 2.

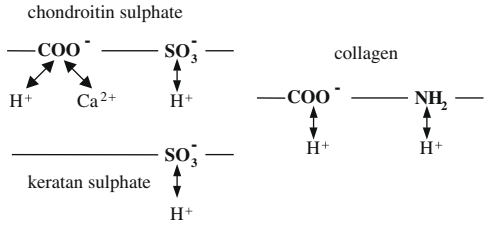

Fig. 2. Acid–base reactions at carboxyl and sulfate sites of GAG's, at carboxyl and amino sites of collagen, and calcium binding at carboxyl sites of GAG's.

The four acid–base reactions involve the weakly acid carboxyl sites of either collagen or PG's, and the strongly acid sulfate sites of PG's,

$$\mathrm{S=CO,SOO}: \qquad \underbrace{\mathrm{S{-}OH}}_{\text{occupied site}} \rightleftharpoons \underbrace{\mathrm{S{-}O^-}}_{\text{free site}} + \underbrace{\mathrm{H^+}}_{\text{fluid phase}}, \tag{3.3}$$

as well as the amino sites of collagen,

$$\mathrm{S=NH_2}: \qquad \underbrace{\mathrm{S\text{-}H^+}}_{\text{occupied site}} \rightleftharpoons \underbrace{\mathrm{S}}_{\text{free site}} + \underbrace{\mathrm{H^+}}_{\text{fluid phase}}. \tag{3.4}$$

In order to compact the notation, the four acid–base reactions are numbered,

$$\mathrm{R}_j \rightleftharpoons \mathrm{P}_j + \mathrm{H}_{(j)}, \quad j \in [1,4], \tag{3.5}$$

with the following conventions for reactants, products and pKs:

S_1 carboxyl sites on PG's	R_1 = CO–OH	P_1 = CO–O^-	$pK_1 = pK_{cg}$
S_2 sulfate sites on PG's	R_2 = SOO–OH	P_2 = SOO–O^-	$pK_2 = pK_{sg}$
S_3 amino sites on collagen	R_3 = NH_2–H^+	P_3 = NH_2	$pK_3 = pK_{ag}$
S_4 carboxyl sites on collagen	R_4 = CO–OH	P_4 = CO–O^-	$pK_4 = pK_{cg}$

Calcium ions compete with hydrogen ions to bind reversibly onto the carboxyl groups of PG's, according to the reaction

$$\underbrace{\mathrm{COO{-}Ca^+}}_{\text{occupied PG's site}} \rightleftharpoons \underbrace{\mathrm{COO^-}}_{\text{free PG's site}} + \underbrace{\mathrm{Ca^{2+}}}_{\text{fluid phase}}. \tag{3.6}$$

The reaction is numbered 1′, and according to the conventions above

$$\mathrm{S_{1'}\ carboxyl\ sites\ on\ PG's}\quad \mathrm{R_{1'}=COO{-}Ca^+}\quad \mathrm{P_{1'}=CO{-}O^-}\quad \mathrm{pK_{1'}=pK_{Ca}}$$

The concentrations at the sites for acid–base reactions and calcium binding may be partitioned in the following general format:

$$\underbrace{c_{\mathrm{S}_j}}_{\text{sites}} = \underbrace{c_{\mathrm{R}_j}}_{\substack{\text{sites occupied}\\ \text{by hydrogen ions}}} + \underbrace{c_{\mathrm{R}_{j'}}}_{\substack{\text{sites occupied}\\ \text{by calcium ions}}} + \underbrace{c_{\mathrm{P}_j}}_{\text{free sites}}, \quad j \in [1,4]. \tag{3.7}$$

For each reaction, the variations in the number of moles of reactants and products obey the relation,

$$\delta N_{\mathrm{XE}_{(j)}} = \delta N_{\mathrm{P}_j} = -\delta N_{\mathrm{R}_j}, \quad j \in [1,4] \cup \{1'\}. \tag{3.8}$$

Here, X stands for H if $j \in [1,4]$, and for Ca if $j = 1'$. The chemical affinities associated with the reactions,

$$\mathscr{G}_j = RT \ln \frac{c_{\mathrm{P}_j}}{c_{\mathrm{R}_j}} \frac{c_{\mathrm{XE}}}{10^{-\mathrm{pK}_j}}, \quad j \in [1,4] \cup \{1'\}, \tag{3.9}$$

are defined in terms of a pK = pK_j, or, equivalently by an enthalpy of formation $\mathscr{G}_j^0 = RT \ln\left(10^{\mathrm{pK}_j} \big/ \hat{v}_{\mathrm{w}}\right)$. Since $c_{\mathrm{HE}} = 10^{-\mathrm{pH_E}}$ for $j \in [1,4]$, the pK_j is seen to be the pH_E at which the numbers of occupied and free sites for the acid–base reaction j are equal at equilibrium, namely for $\mathscr{G}_j = 0$. Similarly, with $c_{\mathrm{CaE}} = 10^{-\mathrm{pCa_E}}$, the $pK_{1'}$ is seen to be the pCa_E at which the numbers of occupied and free sites for calcium binding are equal at equilibrium.

The pKs of the sulfate, carboxyl and amino groups are taken equal to 2, 3.2 and 9.2, respectively. Therefore, since it contains amino acids with carboxyl groups and amino groups, collagen is expected to become charged at pH smaller than 4 or larger than 8, as indicated by Fig. 1. On the other hand, the equilibrium constant $pK_{1'} = pK_{Ca}$ for calcium binding is not known. A parameter analysis from $pK_{Ca} = -\infty$ (no binding) to $pK_{Ca} = 3$ has been observed to increase the IEP from 2.6 to 3.5 for an extrafibrillar calcium concentration lower than 10 mM (Loret and Simões, 2010).

3.3. Site concentrations and electric charge

It is instrumental to introduce the relative concentrations associated with the acid–base reactions,

$$\alpha_j = 10^{\mathrm{pK}_j - \mathrm{pH_E}}, \quad j \in [1,4], \tag{3.10}$$

and with calcium binding,

$$\alpha_j = 10^{\mathrm{pK}_j - \mathrm{pCa_E}} I_{j1'}, \quad j \in [1',4']. \tag{3.11}$$

At equilibrium of the acid–base reactions $\mathscr{G}_j = 0$, $j \in [1,4]$, and of calcium binding $\mathscr{G}_{1'} = 0$, the relative concentrations of the free sites $c_{\mathrm{P}_j}/c_{\mathrm{S}_j}$ and occupied sites $c_{\mathrm{R}_j}/c_{\mathrm{S}_j}$ and $c_{\mathrm{R}_{j'}}/c_{\mathrm{S}_j}$ express in terms of the concentrations of hydrogen and calcium ions, namely for $j \in [1,4]$,

$$\frac{c_{\mathrm{P}_j}}{c_{\mathrm{S}_j}} = \frac{1}{1+\alpha_j+\alpha_{j'}}, \quad \frac{c_{\mathrm{R}_j}}{c_{\mathrm{S}_j}} = \frac{\alpha_j}{1+\alpha_j+\alpha_{j'}}, \quad \frac{c_{\mathrm{R}_{j'}}}{c_{\mathrm{S}_j}} = \frac{\alpha_{j'}}{1+\alpha_j+\alpha_{j'}}. \tag{3.12}$$

The concentration of electric charge,

$$e_{\mathrm{e}} = -c_{\mathrm{P}_1} - c_{\mathrm{P}_2} + c_{\mathrm{R}_3} - c_{\mathrm{P}_4} + c_{\mathrm{R}_{1'}}, \tag{3.13}$$

thus depends on the concentrations of hydrogen and calcium ions via the α's.

3.4. Structure of the constitutive equations

All species in the extrafibrillar phase can exchange with the surroundings but PG's. Let $E_{\mathrm{ext}} = E - \{\mathrm{PG}\}$ denote the set of exchangeable species.

The extrafibrillar hydrogen ions participate to five independent reactions, namely exchange with the surroundings (bath), and four internal acid–base reactions, so that the variation of their mole number is the sum of five contributions,

$$\delta\mathscr{N}_{\mathrm{HE}} = \delta\mathscr{N}^*_{\mathrm{HE}} + \sum_{j\in[1,4]} \delta\mathscr{N}_{\mathrm{HE}_{(j)}}. \tag{3.14}$$

Similarly, extrafibrillar calcium ions exchange with the surroundings and react with PG's,

$$\delta\mathscr{N}_{\mathrm{CaE}} = \delta\mathscr{N}^*_{\mathrm{CaE}} + \delta\mathscr{N}_{\mathrm{CaE}_{(1')}}. \tag{3.15}$$

An additional mechanism should be accounted for if exchanges with the intrafibrillar compartment were activated.

The mole content of the extrafibrillar electric charge can be calculated directly as,

$$\delta\mathscr{N}_{\mathrm{e}} = -\delta\mathscr{N}_{\mathrm{P}_1} - \delta\mathscr{N}_{\mathrm{P}_2} + \delta\mathscr{N}_{\mathrm{R}_3} - \delta\mathscr{N}_{\mathrm{P}_4} + \delta\mathscr{N}_{\mathrm{R}_{1'}} = -\sum_{j\in[1,4]\cup\{1'\}} \delta\mathscr{N}_{\mathrm{XE}_{(j)}}, \tag{3.16}$$

in view of (3.8).

Since the acid–base reactions and calcium binding are electrically neutral, the variation of the electrical density can be expressed in terms of the sole exchanges with the surroundings,

$$\delta I_{\mathrm{eE}} = \mathrm{F}\sum_{l\in E_{\mathrm{ext}}} \zeta_l \delta \mathscr{N}^*_{l\mathrm{E}}. \tag{3.17}$$

The electroneutrality constraint $\delta I_{\mathrm{eE}} = 0$ will be satisfied by introduction of a Lagrange multiplier to be interpreted as the electrical potential ϕ_{E}.

The volume occupied by ions solvated or bound to the solid sites is assumed to be the same. Therefore, since all constituents are incompressible, the condition of compatibility of volume change of the porous medium expresses in the incremental format,

$$\delta I_{\mathrm{Inc}} = \det \mathbf{F}\ \mathrm{tr}\left(\delta\mathbf{F}\cdot\mathbf{F}^{-1}\right) - \sum_{l\in E_{\mathrm{ext}}} \hat{v}_l \delta \mathscr{N}^*_{l\mathrm{E}} = 0. \tag{3.18}$$

This constraint is satisfied by introduction of a second Lagrange multiplier to be interpreted as the pressure p_{E} in the fluid phase.

Along (3.1), the work done in a volume V_0 during an incremental process is thus

$$\begin{aligned}\delta\mathscr{W} &= \mathbf{T}:\delta\mathbf{E} + \sum_{l\in E_{\mathrm{ext}}} g_{l\mathrm{E}}\delta\mathscr{N}^*_{l\mathrm{E}} + \sum_{j\in[1,4]\cup\{1'\}} \mathscr{G}_j \delta\mathscr{N}_{\mathrm{XE}_{(j)}} + p_{\mathrm{E}}\delta I_{\mathrm{inc}} + \phi_{\mathrm{E}}\delta I_{\mathrm{eE}} \\ &= \overline{\mathbf{T}}:\delta\mathbf{E} + \sum_{l\in E_{\mathrm{ext}}} \bar{g}^{\mathrm{ec}}_{l\mathrm{E}}\delta\mathscr{N}^*_{l\mathrm{E}} + \sum_{j\in[1,4]\cup\{1'\}} \mathscr{G}_j \delta\mathscr{N}_{\mathrm{XE}_{(j)}},\end{aligned} \tag{3.19}$$

where $g_{l\mathrm{E}}$ denotes the chemical potential, as opposed to the electro-chemical potential $g^{\mathrm{ec}}_{l\mathrm{E}}$, and the overlined quantities are shifted through the fluid pressure,

$$\overline{\mathbf{T}} = \mathbf{T} + p_{\mathrm{E}}\det\mathbf{F}\ \mathbf{F}^{-1}\cdot\mathbf{F}^{-\mathrm{T}};\quad \bar{g}^{\mathrm{ec}}_{l\mathrm{E}} = g_{l\mathrm{E}} + \mathrm{F}\zeta_k\phi_{\mathrm{E}} - \hat{v}_l p_{\mathrm{E}},\qquad l\in E_{\mathrm{ext}}. \tag{3.20}$$

The set of independent variables $\mathbb{V}_{\mathrm{E}}$ consists of the strain $\mathbf{E}$ of the solid skeleton (or porous medium), of the set of mole contents of chemical species $\mathbb{N}_{\mathrm{E}}$,

$$\mathbb{N}_{\mathrm{E}} = \left\{\mathscr{N}^*_{l\mathrm{E}}, l\in E_{\mathrm{ext}}\right\}\cup\left\{\mathscr{N}_{\mathrm{XE}_{(j)}}, j\in[1,4]\cup\{1'\}\right\}, \tag{3.21}$$

and of the fluid pressure p_{E} and extrafibrillar electrical potential ϕ_{E}.

Hence the coupled chemo-hyperelastic constitutive equations can be cast in the format,

$$\overline{\mathbf{T}} = \frac{\partial\mathscr{W}}{\partial\mathbf{E}};\quad \bar{g}^{\mathrm{ec}}_{l\mathrm{E}} = \frac{\partial\mathscr{W}}{\partial\mathscr{N}^*_{l\mathrm{E}}},\quad l\in E_{\mathrm{ext}};\quad \mathscr{G}_j = \frac{\partial\mathscr{W}}{\partial\mathscr{N}_{\mathrm{XE}_{(j)}}},\quad j\in[1,4]\cup\{1'\}, \tag{3.22}$$

subject to the constraints,

$$I_{\mathrm{inc}} = \frac{\partial\mathscr{W}}{\partial p_{\mathrm{E}}} = 0;\quad I_{\mathrm{eE}} = \frac{\partial\mathscr{W}}{\partial\phi_{\mathrm{E}}} = 0. \tag{3.23}$$

Note that the work-conjugate variables include

- a mechanical couple, involving a stress and a strain;
- as many chemical couples (electro-chemical potential, mole content) as there are species that exchange matter with the surroundings;
- as many chemical couples (chemical affinity, mole content) as there are chemical reactions.

The potential

$$\begin{aligned}\mathscr{W}(\mathbf{E},\mathbb{N}_{\mathrm{E}},p_{\mathrm{E}},\phi_{\mathrm{E}}) &= \mathscr{W}_{\text{ch-mech}}(\mathbf{E},\mathbb{N}_{\mathrm{E}}) + \mathscr{W}_{\mathrm{ch}}(\mathbb{N}_{\mathrm{E}}) + \mathscr{W}_{\mathrm{ef}}(\mathbb{N}_{\mathrm{E}}) \\ &\quad + p_{\mathrm{E}}I_{\mathrm{inc}} + \phi_{\mathrm{E}}I_{\mathrm{eE}},\end{aligned} \tag{3.24}$$

is constitutively decomposed into

- a coupled chemo-mechanical contribution,

$$\mathscr{W}_{\text{ch-mech}}(\mathbf{E},\mathbb{N}_{\mathrm{E}}); \tag{3.25}$$

- a chemical contribution,

$$\begin{aligned}\mathscr{W}_{\mathrm{ch}}(\mathbb{N}_{\mathrm{E}}) = RT\Bigg(&\sum_{l\in E_{\mathrm{ext}}} \mathscr{N}_{l\mathrm{E}}\ln N_{l\mathrm{E}} - \mathscr{N}_{\mathrm{E}}\ln N_{\mathrm{E}} \\ &+ \sum_{j\in[1,4]\cup\{1'\}} \mathscr{N}_{\mathrm{P}_j}\ln N_{\mathrm{P}_j} + \mathscr{N}_{\mathrm{R}_j}\ln N_{\mathrm{R}_j}\Bigg),\end{aligned} \tag{3.26}$$

with

$$\mathscr{N}_{\mathrm{E}} = \sum_{l\in E_{\mathrm{ext}}} \mathscr{N}_{l\mathrm{E}}; \tag{3.27}$$

- a term describing the enthalpies of formation,

$$\mathscr{W}_{\mathrm{ef}}(\mathbb{N}_{\mathrm{E}}) = \sum_{j\in[1,4]\cup\{1'\}} \mathscr{G}^0_j \mathscr{N}_{\mathrm{XE}_{(j)}}, \tag{3.28}$$

with $\mathscr{G}^0_j = RT\ln(10^{\mathrm{pK}_j}/\hat{v}_{\mathrm{w}}), j\in[1,4]\cup\{1'\}$;

- terms intended to ensure satisfaction of the constraints.

The constitutive equations (3.22) can be recast in terms of Cauchy stress in the format,

$$\begin{aligned}&\boldsymbol{\sigma} = -p_{\mathrm{E}}\mathbf{I} + (\det\mathbf{F})^{-1}\mathbf{F}\cdot\frac{\partial\mathscr{W}_{\text{ch-mech}}}{\partial\mathbf{E}}\cdot\mathbf{F}^{\mathrm{T}}, \\ &g^{\mathrm{ec}}_{l\mathrm{E}} = \hat{v}_l p_{\mathrm{E}} + \frac{\partial\mathscr{W}_{\text{ch-mech}}}{\partial\mathscr{N}_{l\mathrm{E}}} + RT\ln x_{l\mathrm{E}} + \mathrm{F}\zeta_l\phi_{\mathrm{E}},\quad l\in E_{\mathrm{ext}} - \{\mathrm{H}\} - \{\mathrm{Ca}\}, \\ &g^{\mathrm{ec}}_{\mathrm{HE}} = \hat{v}_{\mathrm{H}} p_{\mathrm{E}} + \frac{\partial\mathscr{W}_{\text{ch-mech}}}{\partial\mathscr{N}^*_{\mathrm{HE}}} + RT\ln x_{\mathrm{HE}} + \mathrm{F}\phi_{\mathrm{E}}, \\ &g^{\mathrm{ec}}_{\mathrm{CaE}} = \hat{v}_{\mathrm{Ca}} p_{\mathrm{E}} + \frac{\partial\mathscr{W}_{\text{ch-mech}}}{\partial\mathscr{N}^*_{\mathrm{CaE}}} + RT\ln x_{\mathrm{CaE}} + 2\mathrm{F}\phi_{\mathrm{E}}, \\ &\mathscr{G}_j = RT\ln\frac{c_{\mathrm{P}_j}}{c_{\mathrm{R}_j}}\frac{c_{\mathrm{XE}}}{10^{-\mathrm{pK}_j}},\quad j\in[1,4]\cup\{1'\},\end{aligned} \tag{3.29}$$

subject to the conditions (3.23) of incompressibility and electroneutrality.

3.5. Equilibria

At the time scale of interest here, the acid–base reactions, as well as the exchanges between the cartilage and the surroundings, are considered at equilibrium. Moreover, it is tacitly understood that all species in the set $\mathrm{E}_{\mathrm{ext}}$ can exchange with the bath, and that the latter contains only these species.

Therefore, the equations that control the chemo-mechanical evolution of the cartilage in contact with a bath of given chemical composition govern

- the exchanges with the surroundings:

$$g^{\mathrm{ec}}_{l\mathrm{E}} = g^{\mathrm{ec}}_{l\mathrm{B}},\quad l\in E_{\mathrm{ext}}; \tag{3.30}$$

- the acid–base reactions, and calcium binding:

$$\mathscr{G}_j = 0,\quad j\in[1,4]\cup\{1'\}; \tag{3.31}$$

- the compatibility of molar fractions,

$$\sum_{l\in\mathrm{K}} x_{l\mathrm{K}} = 1,\quad \mathrm{K} = \mathrm{E},\mathrm{B}; \tag{3.32}$$

- the electroneutrality condition in terms of the molar fraction $y_{\mathrm{e}} = \hat{v}_{\mathrm{w}} e_{\mathrm{e}}$,

$$x_{\mathrm{NaK}} + 2x_{\mathrm{CaK}} + y_{\mathrm{e}} I_{\mathrm{KE}} + x_{\mathrm{HK}} - x_{\mathrm{OHK}} - x_{\mathrm{ClK}} = 0,\quad \mathrm{K} = \mathrm{E},\mathrm{B}; \tag{3.33}$$

- water dissociation in terms of molar fractions,

$$x_{\mathrm{HK}}x_{\mathrm{OHK}} = 4\times10^{-18},\quad \mathrm{K} = \mathrm{E},\mathrm{B}. \tag{3.34}$$

The condition of mechanical equilibrium should be added to the above to close the problem.

The electro-chemical potentials of the species in the cartilage are provided by the constitutive equations developed above while the expressions for the species in the bath are given by (3.2).

4. Chemically induced stiffening/softening by fiber recruitment/deactivation

At physiological pH, the compressive stiffness of articular cartilages is contributed mostly by the ground substance, via the electrical repulsion between charged GAG's. The collagen network contributes as well at non-physiological pHs. Indeed, at low and high pH's, the collagen molecules are charged, and their repulsion contributes to a significant compressive stiffness.

The tensile stiffness is provided by the ground substance and mostly by collagen fibrils. Under an extension, the fibers progressively uncrimp, so as to carry the tensile load. They can be considered fully activated if their extension is larger than some characteristic value. Fibers aligned with a tensile load are certainly in extension, while fibers along orthogonal directions are likely to undergo contraction, and therefore to be mechanically inactive.

Emphasis is laid below on the interactions between the directional properties of the fiber network, and chemo-mechanical couplings. The model displays *a swelling induced stiffening* by fiber recruitment, and, conversely, *a shrinking induced softening* by fiber deactivation.

Indeed, consider the material to undergo uniaxial traction, while swelling emanates from some chemo-mechanical process. Swelling will imply the lateral strains to become less contractive. Therefore, more collagen fibrils will be activated. Consequently, the axial stiffness is certainly going to increase. Simulations will show that this inherent stiffening/softening effect is significant.

To simplify the analysis, full activation of individual fibers is considered to take place as soon as the fibers undergo an extension. Progressive uncrimping is introduced through a nonlinear stress strain relation.

4.1. A single family of collagen fibrils

The unit vector $\mathbf{m}_c$, indicating the direction of a collagen fiber in the reference configuration where $\mathbf{F} = \mathbf{I}$ is expressed in terms of the angles $\alpha \in [0, 2\pi[$ and $\beta \in [0, \pi[$, Fig. 3. Let $\mathbf{M}_c = \mathbf{m}_c \otimes \mathbf{m}_c$.

The collagen fibrils are mechanically active only in extension, namely when $\langle \mathbf{m}_c \cdot \mathbf{C} \cdot \mathbf{m}_c - 1 \rangle$ is non-zero, where $\mathbf{C} = \mathbf{F}^T \cdot \mathbf{F}$ is the right stretch associated with the deformation gradient $\mathbf{F}$, and the operator $\langle \cdot \rangle$ denotes the positive part of its argument. Then the strain energy of a fiber expresses in terms of the right stretch or Green strain $\mathbf{E} = (\mathbf{C} - \mathbf{I})/2$ in the format,

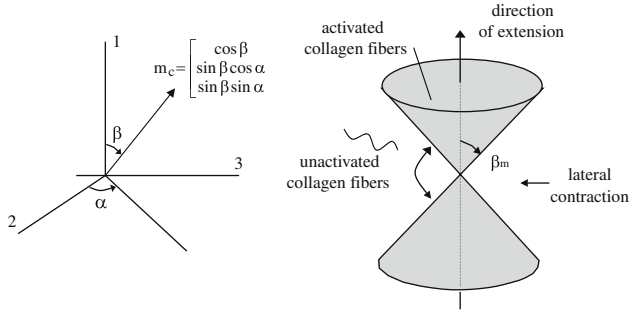

Fig. 3. Cones of activation of collagen fibrils in axial extension and lateral contraction.

$$w^c = w^c(X^2), \tag{4.1}$$

where

$$X = \frac{1}{2}\langle \mathbf{C} : \mathbf{M}_c - 1 \rangle = \langle \mathbf{E} : \mathbf{M}_c \rangle. \tag{4.2}$$

In (4.1), the square, actually any power strictly greater than 1, is required to ensure continuity of the stress at the extension-contraction transition, where, in contrast, the stiffness may, or may not, be discontinuous. Note that use of the deviatoric deformation in the above energy would lead isotropic extension, like swelling, to leave collagen fibrils unactivated. The exponential form of energy, defined by the modulus K_c (unit: MPa) and the dimensionless exponent k_c, is adopted,

$$\begin{aligned} w^c &= \frac{K_c}{2k_c}\Big(\exp(k_c X^2) - 1\Big), \\ \frac{\partial w^c}{\partial \mathbf{E}} &= K_c \exp(k_c X^2)\, X \mathbf{M}_c, \\ \frac{\partial^2 w^c}{\partial \mathbf{E} \partial \mathbf{E}} &= K_c \exp(k_c X^2)\left(2k_c \underbrace{X^2}_{\text{continuous}} + \underbrace{\mathscr{H}(\mathbf{E} : \mathbf{M}_c)}_{\text{discontinuous}}\right)\mathbf{M}_c \otimes \mathbf{M}_c. \end{aligned} \tag{4.3}$$

4.2. The stress of the collagen network

Henceforth, we have in mind a collagen piece taken in the middle zone, as in Grodzinsky et al. (1981), so that the directional distribution of collagen fibrils $\Phi(\alpha, \beta)$ can be assumed to be uniform, namely $4\pi\Phi(\alpha, \beta) = 1$. Nevertheless, the influence of a non-isotropic directional distribution of collagen fibrils has been tested. As an additional simplification, the fibers are considered to be independent, namely there are no crosslinks between fibers, nor interaction with the matrix.

The strain energy, obtained by integration over the unit sphere Ω^3,

$$\mathscr{W}^c(\mathbf{E}) = \int_{\Omega^3} w^c(X)\Phi(\alpha, \beta)\, d\Omega, \tag{4.4}$$

provides the stress of the collagen network,

$$\mathbf{T}^c = \frac{\partial \mathscr{W}^c(\mathbf{E})}{\partial \mathbf{E}} = K_c \int_{\Omega^3} X \exp(k_c X^2)\mathbf{M}_c \Phi(\alpha, \beta)\, d\Omega. \tag{4.5}$$

If the directional distribution of collagen fibrils shows a rotational symmetry about the axis 1, so that $\Phi = \Phi(\beta)$, then the stress components can be cast in the format,

$$T^c_{ij} = K_c \int_0^{\pi/2} d\beta \sin\beta X \exp(k_c X^2) 4\pi\Phi(\beta) \begin{cases} (\cos\beta)^2, & i = j = 1; \\ (\sin\beta)^2/2, & i = j = 2, 3; \\ 0, & i \neq j. \end{cases} \tag{4.6}$$

For uniaxial traction along the symmetry axis 1, the activation criterion relies on the elongation X,

$$X = \langle \mathbf{E} : \mathbf{M}_c \rangle = \Big\langle E_{11}(\cos\beta)^2 + E_{22}(\sin\beta)^2 \Big\rangle. \tag{4.7}$$

In general, the directions for which extension takes place are not known beforehand, and the integration cannot be performed analytically, except in particular cases. Of course, if the transverse directions 2 and 3 undergo extension, an isotropic response is recovered. If the transverse directions undergo contraction, then the fibers which undergo extension $\mathbf{E}{:}\mathbf{M}_c \geqslant 0$, namely,

$$\cot^2\beta = \frac{m_1^2}{m_2^2 + m_3^2} \geqslant \cot^2\beta_m \equiv \frac{-E_{22}}{E_{11}}, \tag{4.8}$$

form, as sketched in Fig. 3, two symmetric cones of half angle β_m about the extension direction,

$$\beta \in [0, \beta_m] \cup [\pi - \beta_m, \pi]. \tag{4.9}$$

4.3. Elastic potential with electro-chemo-mechanical couplings

The general framework developed in Section 3 is now specialized so as to simulate intermingled chemical and mechanical loading paths available in the literature. These data unambiguously show the strong influence of ionic strength and pH on the material response. However, since no sufficient information on the articular cartilage tested is available, only a prototype of mechanical model can be formulated.

The chemo-mechanical part of the elastic potential

$$\mathscr{W}_{\text{ch-mech}}(\mathbf{E}, \mathbb{N}_E) = \mathscr{W}_{\text{ch},1}(\mathbf{E}, \mathbb{N}_E) + \mathscr{W}_{\text{ch},2}(\mathbb{N}_E)(\mathscr{W}^{\text{gs}}(\mathbf{E}) + \mathscr{W}^{\text{c}}(\mathbf{E})), \tag{4.10}$$

is contributed by

- the mechanical energy $\mathscr{W}^{\text{gs}}(\mathbf{E})$ of the matrix, PG's and other proteins (ground substance);
- the mechanical energy $\mathscr{W}^{\text{c}}(\mathbf{E})$ of the activated collagen fibrils;
- a coupled chemo-mechanical term $\mathscr{W}_{\text{ch},1}(\mathbf{E}, \mathbb{N}_E) = -p_{\text{ch}}(\mathbb{N}_E)(\det \mathbf{F} - 1)$, and a purely chemical term $\mathscr{W}_{\text{ch},2}(\mathbb{N}_E)$.

The coupled chemo-mechanical term gives rise to the chemical stress $\mathbf{T}_{\text{ch}} = -p_{\text{ch}} \det \mathbf{F}\, \mathbf{F}^{-1} \cdot \mathbf{F}^{-\text{T}}$ which results in an isotropic Cauchy stress $\boldsymbol{\sigma}_{\text{ch}} = -p_{\text{ch}}\mathbf{I}$.

The constitutive stresses of the ground substance $\mathbf{T}^{\text{gs}} = \partial \mathscr{W}^{\text{gs}}/\partial \mathbf{E}$ and of the collagen $\mathbf{T}^{\text{c}} = \partial \mathscr{W}^{\text{c}}/\partial \mathbf{E}$ are to be understood as volume weighted averages. Moreover, both are representative of the stresses of the matrix and collagen in the hypertonic state, that is, in absence of chemical effects.

With $\boldsymbol{\sigma}^{\text{gs}}$ and $\boldsymbol{\sigma}^{\text{c}}$ the Cauchy stresses associated with the second Piola–Kirchhoff stresses $\mathbf{T}^{\text{gs}}$ and $\mathbf{T}^{\text{c}}$, the mechanical constitutive equations (3.29) may be phrased in terms of an effective stress in the current configuration,

$$\boldsymbol{\sigma} + \overbrace{(p_E + p_{\text{ch}})}^{p_{\text{eff}}}\mathbf{I} = \mathscr{W}_{\text{ch},2}(\mathbb{N}_E)(\boldsymbol{\sigma}^{\text{gs}} + \boldsymbol{\sigma}^{\text{c}}). \tag{4.11}$$

The second chemical term $\mathscr{W}_{\text{ch},2}$ is intended to indicate that a smaller ionic strength amplifies the stiffness, both in confined compression, and in uniaxial traction (Loret and Simões, 2004, Fig. 5).

The cartilage specimen is assumed to be in equilibrium with a fictitious bath at pressure $\tilde{p}_E$. The constitutive equation (4.11) is then rewritten in the format,

$$\boldsymbol{\sigma} + \tilde{p}_E\mathbf{I} + (\pi_{\text{osm}} + p_{\text{ch}})\mathbf{I} = \mathscr{W}_{\text{ch},2}(\mathbb{N}_E)(\boldsymbol{\sigma}^{\text{gs}} + \boldsymbol{\sigma}^{\text{c}}), \tag{4.12}$$

that involves the osmotic pressure $\pi_{\text{osm}} = p_E - \tilde{p}_E$. The properties of the fictitious bath are deduced from those of the cartilage. Therefore, the osmotic pressure can be seen as a function of the state variables. It consequently qualifies to enter the constitutive equations.

For a general boundary value problem, the indeterminate pressure p_E is defined by boundary conditions. Here, we consider a homogeneous specimen in equilibrium with a (real) bath. Therefore, the fictitious bath and the real bath can be identified, $\tilde{p}_E$ is understood as the pressure p_B of the real bath, chemical equilibrium provides π_{osm}, and then the pressure in the cartilage p_E is equal to $\pi_{\text{osm}} + \tilde{p}_E$.

4.4. Material parameters

In the hypertonic state, the high ionic strength shields quasi-completely the electro-chemical repulsion forces between fixed charges of identical sign. The hypertonic state is therefore a likely candidate as a reference state.

4.4.1. Hypertonic elastic coefficients

The moduli that come into picture should be apparent moduli. The apparent isotropic tensor moduli $\mathbb{E}^{\text{gs}}$ of the matrix are defined by the Lamé moduli $\lambda = n^{\text{gs}}\Lambda_{\text{gs}}$ and $\mu = n^{\text{gs}}M_{\text{gs}}$ built from the intrinsic moduli of the matrix Λ_{gs} and M_{gs}, and its volume fraction n^{gs}. The order of magnitude of the moduli of the ground substance in the hypertonic state can be estimated from the confined compression tests of Eisenberg and Grodzinsky (1985), namely $\lambda = \mu = 100$ kPa.

The modulus of collagen fibrils of bovine Achilles tendons is reported to be 430 MPa by Sasaki and Odajima (1996). Lower values are mentioned for collagen fibrils (of type I) of annulus fibrosus, namely about 50 MPa (Pezowicz et al., 2005). Federico et al. (2005) report values from Athanasiou et al. (1991) about 10 MPa for articular cartilages. For collagen, the volume fraction n^{c} is expressed as the product of the volume fraction of the fluid phase $n^E = 0.8$, times the concentration of collagen with respect to the fluid phase $c_c = 0.8$ mole/m^3, times the molar volume of collagen $\hat{v}_c = 0.2$ m^3/mole, and therefore, $n^c = 0.128$. The simulations have been run with a modulus $K_c = n^c\Lambda_c = 1$ MPa and an exponent $k_c = 100$. At low ionic strength, these values yield an axial stress of about 1 MPa for an axial strain of 15%, in agreement with measurements on human knees by Akizuki et al. (1986).

4.4.2. Identification of the constants of the chemo-mechanical couplings

The constitutive chemo-mechanical couplings are motivated by the following remarks:

- Sodium cations Na^+ and chloride anions Cl^- have only shielding effect in articular cartilage, screening the repulsion between fixed charges of identical sign located on the PG's and collagen.
- Calcium ions Ca^{2+} display the shielding effect, which should be more efficient that sodium ions due to the valence 2, and in addition they increase the algebraic value of the charge, through binding to carboxyl sites of PG's. These two effects cooperate above the isoelectric point (IEP), and compete below the IEP. Note however that binding concerns only part of the sites, and, calcium binding cannot by itself alone change the sign of the fixed charge.
- Ions hydrogen both shield the charge and bind to the PG's and collagen sites, and are able to change the sign of the fixed charge.

The osmotic pressure is large at low ionic strength, and vanishes at large ionic strength and at the IEP. It is therefore a likely candidate to carry the extremum properties that are expected for the constitutive function $\mathscr{W}_{\text{ch},2}$, which adopts a simple affine relation,

$$\mathscr{W}_{\text{ch},2} = 1 + \alpha_w \pi_{\text{osm}}/\pi^0_{\text{osm}}, \tag{4.13}$$

where α_w is a dimensionless constant. n^E and n^E_0 are, respectively, the current and reference fluid volume fractions. π^0_{osm} is the osmotic pressure induced by isotropic free swelling, up to 10^{-4} M of NaCl at $pH_B = 7$: it is found equal to about 325 kPa. In absence of sufficient data, the chemo-mechanical term is neglected, i.e. $p_{\text{ch}} = 0$.

Assume the material to be strained, subsequent to isotropic free swelling, at fixed bath chemical composition. Then (4.12) writes at any state,

$$\sigma_{11} + \tilde{p}_E = \mathscr{W}_{ch,2}(\sigma_{11}^{gs} + \sigma_{11}^{c}) - (\pi_{osm} + p_{ch}). \tag{4.14}$$

In the tests to be described below, the only data that are available are the ratios between the l.h.s. of (4.14) at a current state over the value at a certain stage of the loading history. The coefficient $\alpha_w = 10$ in (4.14) implies these stress ratios to be about 1/4 in the hypertonic state in agreement with data, and the isotropic free swelling strain to be about 4%.

5. Simulations of tests on articular cartilages

Cartilage strips cut from bovine femoropatellar joints, of 1.5- to 2-year-old animals, were tested by Grodzinsky et al. (1981). Since the strips are taken from the middle zone, the collagen fibrils can be assumed to be randomly distributed over all spatial directions.

The cartilage specimens, in contact with a bath of controlled chemical composition, are subjected to intermingled chemical and mechanical loadings. The complete simulations start from a hypertonic state in presence of sodium cations at 1 M, and involve three sequences, as sketched in Fig. 4: namely

- *Sequence 1*: isotropic free swelling OA, i.e. progressive decrease of the ionic strength of sodium of the bath from pNaB = 0 to pNaB = 4.
- *Sequence 2*: uniaxial traction at fixed bath composition AB, i.e. application of an additional axial strain of 10%.
- *Sequence 3*: chemical loading BC, i.e. increase of the ionic strength of the bath, while the axial strain is maintained constant. Since the lateral strains vary, the test is actually not isometric.

As an extension of the notion of pH, data are reported as a function of the $pk_B = -\log_{10} c_{kB}$ of the bath, the concentration $c_{kB} = 10^{-pk_B}$ being measured in mole/l, with k = Na, Ca, H.

During sequence 1, the pH of the bath is maintained constant, equal to 7, except for the H-test where it is equal to 6.

The third sequence consists in increasing the bath concentrations of sodium chloride (Na-test), calcium chloride (Ca-test), or hydrochloric acid (H-test). For the Na- and Ca-tests, the pH in the bath is maintained equal to 7. For the Na- and H-tests, the amount of calcium is virtually nil. In detail,

- the conditions at B for the Na-test are $pNa_B = 4$, $pH_B = 7$;
- for the Ca-test, the neutralizing cations at B are Na^+, with $pNa_B = 6$, the initial pCa_B is 4, and the initial pH_B is 7;
- for the H-test, the free swelling test stops at concentration of Na^+ equal to 0.06 M, and the pH_B at B is 6.

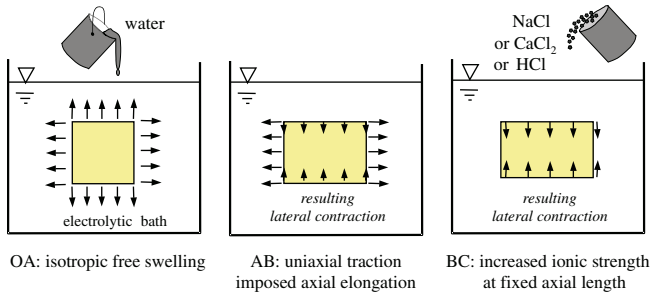

Fig. 4. Scheme of the three sequences of the chemo-mechanical tests to which specimens of articular cartilages are subjected. The electrolytic bath is kept at atmospheric pressure, but its chemical composition is modified in sequences 1 and 3. OA: isotropic free swelling starting from hypertonic state; AB: uniaxial traction at fixed bath chemical composition; BC: increasing ionic strength of the bath at constant axial strain.

For a conewise nonlinear behavior of collagen fibrils, the boundary condition for uniaxial traction along the direction 1,

$$0 = \sigma_{22} + \tilde{p}_E = \mathscr{W}_{ch,2}(\mathbb{N}_E)\left(\sigma_{22}^{gs} + \sigma_{22}^{c}\right) - (\pi_{osm} + p_{ch}), \tag{5.1}$$

becomes an implicit equation for the lateral strain, which has to be solved numerically. Moreover, for a randomly distributed fiber network, isotropic free swelling is recovered by constraining the strain to be isotropic.

The simulations below have been performed with both quadratic and exponential strain energy functions for the collagen fibrils. Unlike mechanical variables, the chemical variables (concentrations, fixed charge, etc.) do not show significant differences for the two models: therefore the mechano-chemical coupling is weak.

Only the nonlinear simulations are presented. They are displayed in Figs. 5–11:

1. During the free swelling sequence OA, at decreasing concentration of Na^+, the pH in the cartilage fluid decreases much, Fig. 9, in agreement with the findings of Loret and Simões (2010). Therefore, the electric fixed charge decreases (in absolute value). On the other hand, decreasing ionic concentration alone would lead to increase of the osmotic pressure. These two competing effects imply the osmotic pressure to show a maximum. The phenomenon is displayed essentially in the Na-test, because the swelling sequence is limited in the H-test. In presence of calcium, the variation of cartilage pH is tiny, and the osmotic pressure does not show such a marked maximum.
2. In the Na-test, the chemical load path is closed, Fig. 5. The concentration of Na^+ in the cartilage returns to its initial value. So do also the other concentrations in the cartilage. This is another indication that the *mechano-chemical coupling is weak*.
3. On the other hand, strain and stress components do not follow a closed path, since the mechanical loading path is not closed, Fig. 6. Further, the mechanical response (stress and strain components) is strongly affected by the chemical loading of sequence 3: this is a witness that the *chemo-mechanical coupling is strong*.
4. During sequence 3, at increasing ionic strength, the stress falls down onto the hypertonic curve at large ionic strength of the bath.
5. However, the decrease is not monotonous for the H-test, because the isoelectric state is reached first, at $pH_B = pH_E = 2.6$. Let us recall that, at the isoelectric point (IEP), the chemical concentrations in the bath and extrafibrillar fluid are virtually identical (to within the tiny concentration of PG's), and therefore the osmotic pressure vanishes. Once the IEP is passed, subsequent decrease of the bath pH implies an increasing positive fixed charge of the collagen network, Fig. 10. This increasing fixed charge and the increasing ionic strength compete to control the magnitude of the stress, which first increases, reaches a local maximum at $pH_B \sim 1$, and finally falls down on to the hypertonic curve at larger ionic strength. In summary, for the H-test, the stress falls down to the hypertonic line twice, first because the fixed charge vanishes at the IEP, and second at large ionic strength, as a consequence of the strong shielding of the electric charge by the mobile ions.
6. The volumetric contraction is maximum in the hypertonic state, which, as already mentioned, is reached either due to a large ionic strength (Na-, Ca- and H-curves) or at the isoelectric point (H-curve).

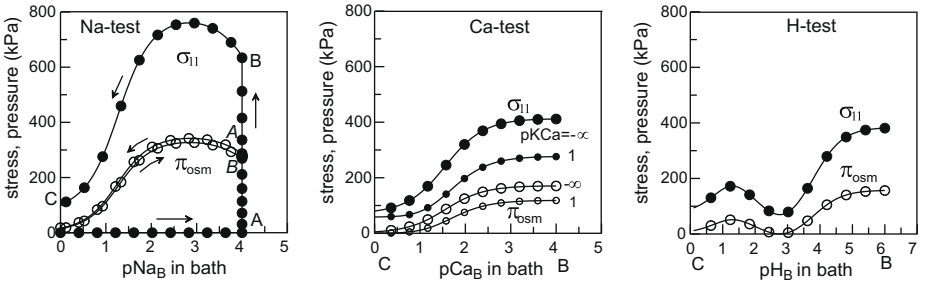

Fig. 5. Simulations of a three sequence loading path. Axial stress and osmotic pressure as a function of the $pk_B = -\log_{10} c_{kB}$ of the bath, the concentration $c_{kB} = 10^{-pk_B}$ being measured in mole/l, with k = Na, Ca, H. The stress reaches the hypertonic value, and the osmotic pressure vanishes, at large ionic strength for the three tests, and in addition at the IEP for the H-test. Binding of calcium is characterized by the constant pKCa, namely pKCa = $-\infty$ (no binding), pKCa = 1 (binding at large concentrations only).

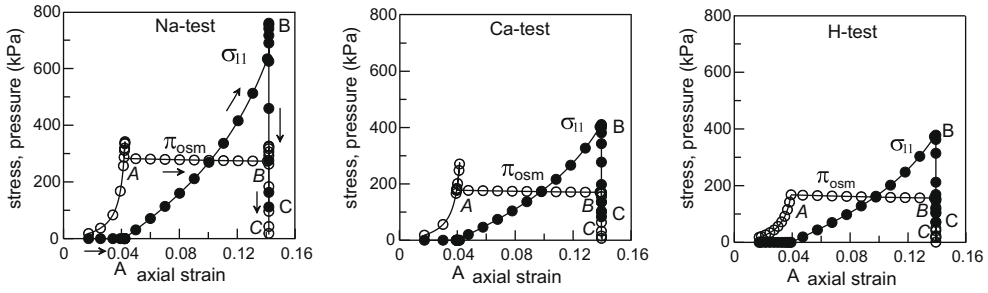

Fig. 6. Same as Fig. 5. Axial stress and osmotic pressure as a function of the axial strain. The stress varies due to mechanical loading AB and chemical loading BC, because the chemo-mechanical coupling is strong, while the osmotic pressure varies essentially due to chemical loadings OA and BC, but little due to mechanical loading because the mechano-chemical coupling is weak.

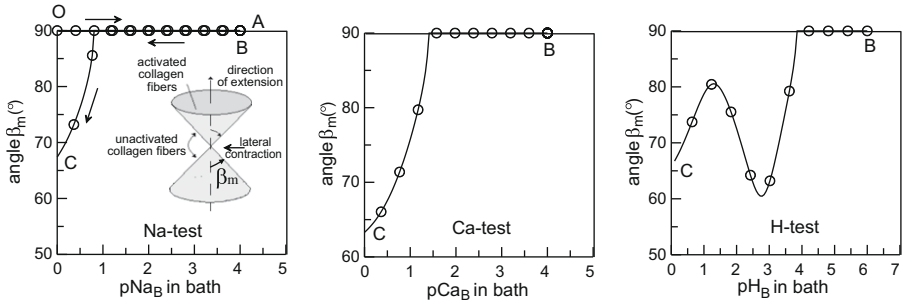

Fig. 7. Same as Fig. 5. Angle β_m defining the cones of fibers in extension as a function of the pk_B of the bath. Lateral contraction during increase of ionic strength BC implies the cones of fibers which undergo extension to shrink. This is another witness of the strong chemo-mechanical coupling.

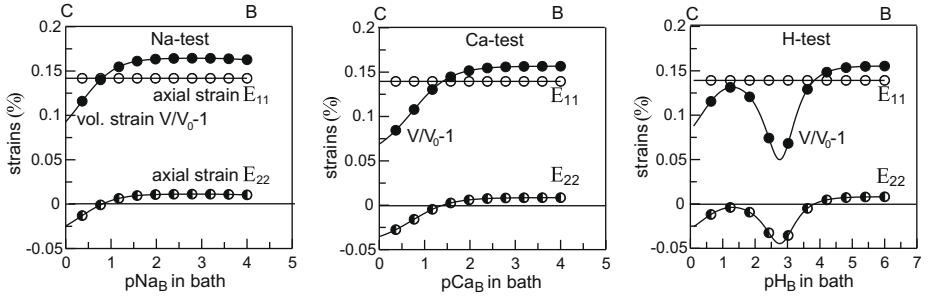

Fig. 8. Same as Fig. 5. Strains as a function of the pk_B of the bath. When the concentration of metallic ions in the bath increases, path BC, the two adverse effects of electrical shielding and increase of fixed charge compete, and the former effect takes over, leading to contraction. The situation is somehow different in the H-test, because the fixed charge changes sign, leading to a non-monotonous evolution of the strains.

7. As indicated by (4.12), during isotropic free swelling, the chemical pressure driven by the electrical repulsion between cartilage units is resisted by both the matrix (PG's) and the collagen network. During uniaxial traction, the latter have to resist, in addition, the external load. In fact, during the swelling sequence 1, all collagen fibrils

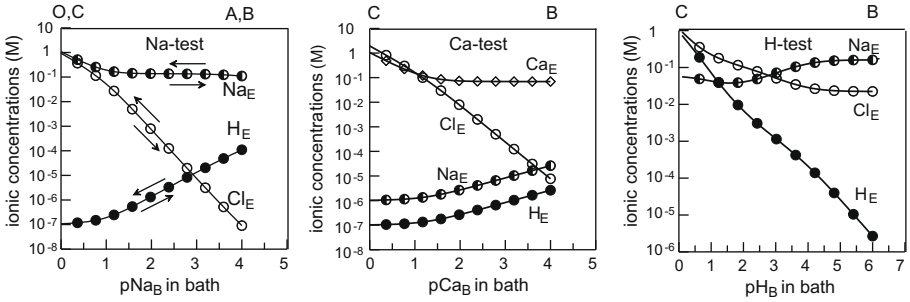

Fig. 9. Same as Fig. 5. Ionic concentrations in the tissue as a function of the pk_B of the bath. In the Na-test, the chemical loading path is closed, while the mechanical loading path is not. Still the ionic concentrations in the cartilage are almost closed as the mechano-chemical coupling is weak. As the concentration in metallic ions of the bath increases, path BC, the cartilage becomes less acidic.

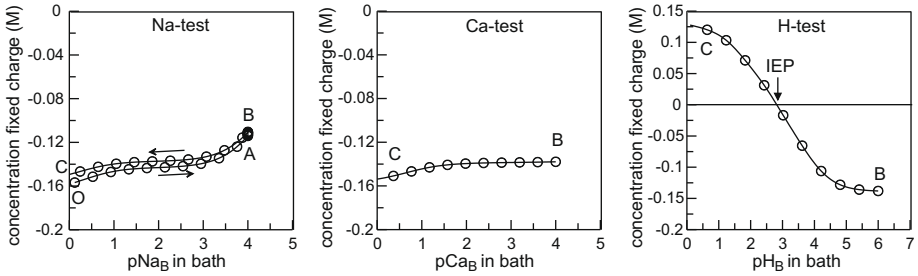

Fig. 10. Same as Fig. 5. Extrafibrillar fixed charge as a function of the pk_B of the bath. As the concentration in metallic ions of the bath increases, path BC, the cartilage becomes less acidic, so that the fixed charge becomes more negative. The opposite takes place when the pH of the bath decreases, and the total fixed charge changes sign at the IEP.

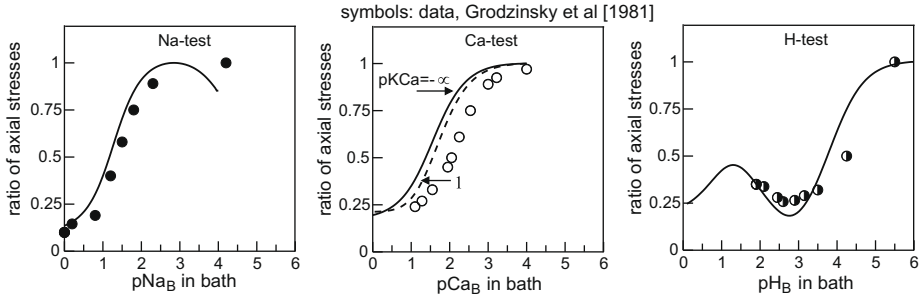

Fig. 11. Axial stress scaled by its maximum value during the third sequence BC. Comparison with data (symbols) by Grodzinsky et al. (1981). While the stress decrease is monotonic and only due to ionic strength for the Na- and Ca-tests, it reaches twice the minimum hypertonic value for the H-curve, once at the isoelectric point, at pH about 2.6, and later as the ionic strength overweighs the presence of the fixed charge.

are in extension, corresponding to an angle $\beta_m = 90°$, Fig. 7. The lateral strain reduces during the traction sequence 2, Fig. 8. This decrease continues during the chemical loading sequence 3, associated with shrinking, which, since the axial strain is fixed, can take place only along the lateral direction. During the last two sequences, the angle β_m decreases progressively, as soon as the lateral strain becomes negative. The actual range of variation β_m depends on the ratio $(\pi_{osm} + p_{ch})/\mathscr{W}_{ch,2}$ which could be estimated from isotropic free swelling; the larger this ratio, the larger the lateral strain, and the larger the angle β_m.

8. The actual mechanical behavior below the IEP may depend both on the loading conditions, and on the structural characteristics of the tissue. For corneal stroma where the IEP is about 4, osmotic pressure and hydration raise considerably for bath pH up to 3, to values larger than at neutral pH (Huang and Meek, 1999). Therefore, in this range of bath pH, electrical repulsion between collagen units is quite efficient. Whether or not the structure collapses at lower pH is not known, and perhaps, not of direct interest here since extreme pHs may induce further modifications to the tissue. These aspects are considered in the next section.
9. Calcium binding to the carboxyl sites of PG's lowers the stress and osmotic pressure, since it reduces the fixed charge, Fig. 5. The influence is not that apparent in the stress ratio of the Ca-test in Fig. 11.
10. The axial stresses relative to their values at the beginning of sequence 3 are the only data provided by Grodzinsky et al. (1981). The simulations show indeed ratios quite in agreement with these data, Fig. 11. However, the simulations seem to indicate a systematic shift at low ionic strength (large pkB), as if the model was overestimating small concentrations. In presence of calcium, binding provides a simulation curve marginally closer to the experimental data.

6. Simulations of tests on corneal stroma

Corneal stroma presents some qualitative similarities with articular cartilages: while the fixed charge is due to PG's at neutral pH, collagen contributes at low and high pHs. On the other hand, while calcium ions compete with hydrogen ions to bind on the carboxyl sites of PG's, the ligands on which chloride ions bind are assumed to be pH independent.

The actual composition and structure of these tissues reflect the fact that their biological functions are quite distinct:

- Collagen fibrils are embedded in lamellae and they run essentially parallel to the corneal surface, and not across the thickness along the radial direction.
- These lamellae are also parallel to the corneal surface, except perhaps close to the limbus. The interlamellar space opens easily due to swelling, by anterior–posterior stretching.
- Therefore, the stroma is hardly able to resist increase of hydration, and, by itself alone, it would swell almost indefinitely, forming lakes that impair transparency (Elliott and Hodson, 1998).
- Infinite swelling is avoided by active transport maintained by pumps located on the endothelium.

Here, we consider a de-epithelized corneal specimen: the ionic pumps have been removed. Its hydration is limited by an applied osmotic pressure through polyethylene glycol (PEG). The model endows the stromal matrix with elastic moduli that are of course larger in compression than in tension: the latter, while small, are to be traced to the sub-lamellae and fibrils connections that run across the lamellae.

The composition of PG's has been extracted from Plaas et al. (2001):

- Numbers of disaccharide units per KS which are unsulfated, monosulfated and disulfated, respectively, 0.56, 5.88 and 7.56.
- Numbers of disaccharide units per CS which are unsulfated and monosulfated, respectively, 25.6 and 14.4.
- Numbers of moles of GAG's of KS and CS per gram of dry mass, respectively, 2.2×10^{-6} and 0.5×10^{-6}.
- Molar masses of GAG's of KS and CS, respectively, 7.0×10^3 and 17.5×10^3.

The chloride binding reaction,

$$\underbrace{\mathrm{L{-}Cl^-}}_{\text{occupied ligand}} \rightleftharpoons \underbrace{\mathrm{L}}_{\text{free ligand}} + \underbrace{\mathrm{Cl^-}}_{\text{fluid phase}}, \tag{6.1}$$

is denoted $j = \mathrm{L}$. Along the conventions used for acid–base reactions,

S_L total ligand sites L on collagen R_L occupied ligands $\mathrm{L{-}Cl^-}$

P_L free ligands L,

the sites for acid–base reactions and chloride binding are partitioned in the format,

$$\underbrace{c_{S_j}}_{\text{sites}} = \underbrace{c_{R_j}}_{\substack{\text{sites occupied}\\ \text{by hydrogen/chloride ions}}} + \underbrace{c_{P_j}}_{\text{free sites}}, \quad j \in [1,4] \cup \{\mathrm{L}\}. \tag{6.2}$$

Further notations similar to the acid–base reactions are introduced, namely, $c_{\mathrm{Cl}\mathrm{E}} = 10^{-\mathrm{pCl_E}}$ with $c_{\mathrm{Cl}\mathrm{E}}$ expressed in mole/l, and $\alpha_L = 10^{\mathrm{pK_L}-\mathrm{pCl_E}}$. Therefore, the concentrations of free ligands c_{P_L}, occupied ligand c_{R_L} and total ligands c_{S_L} are governed by the relations,

$$\frac{c_{P_L}}{c_{S_L}} = \frac{1}{1+\alpha_L}, \quad \frac{c_{R_L}}{c_{S_L}} = \frac{\alpha_L}{1+\alpha_L}. \tag{6.3}$$

Due to chloride binding, the fixed charge concentration is decreased by $-c_{R_L}$. Data on chloride binding are taken from Hodson et al. (1992), namely

- number of ligands per gram of dry mass 0.24 mole/kg;
- equilibrium constant $\mathrm{pK_L} = 0.523$.

Huang and Meek (1999) have submitted to chemical and mechanical loadings bovine corneas, from which endothelium and epithelium were removed by scraping with a scalpel.

As a rough simplification, the mechanical properties of corneal stroma are assumed to be transversely isotropic about the radial direction. The collagen fibrils are orthoradial (parallel to the corneal surface), and uniformly spread over all the tangential directions. This directional distribution is largely approximative, but it does not affect the simulations below where the strains are essentially radial. A more accurate description of the directional distribution of the fibrils would lead to consider a clinotropic material with two main fiber directions. A further refinement would distribute smoothly the fibrils around these two directions.

The chemo-mechanical constitutive equations are essentially similar to those used for articular cartilages. The ground substance (matrix) is endowed with isotropic elastic properties, with Lamé moduli $\lambda_e = 1.5$ kPa for volume increase, $\lambda_c = 6$ kPa for volume decrease and a shear modulus $\mu = 1.5$ kPa. Indeed, the complex loadings to which the stromal specimens are subjected in the experiments reported by Huang and Meek (1999) include both compression stages and stages of volume expansion. While the reported measurements do not allow to accurately backtrack the elastic properties, simulations indicate that the matrix moduli during the swelling phase are much lower than during the compression phase. Within the framework of isotropic elastic materials, such a conewise behavior can be realized by assuming the Lamé modulus λ to be different for volume increase and for volume decrease, while the shear modulus should remain identical. This difference of moduli is to be traced to the lamellar architecture of the stroma, briefly touched upon at the beginning of the section.

The elastic behavior of collagen fibrils is nonlinear, exactly like for articular cartilages, with modulus $K_c = 1000$ kPa and exponent $k_c = 100$. In order to recover the experimental IEP of 4, the collagen charge is fully required to contribute to the extrafibrillar charge. In contrast, for articular cartilages, only two third of the collagen charge was contributing to the extrafibrillar charge.

The chemo-mechanical coupling is introduced only by the osmotic pressure. In absence of sufficient data, the chemical pressure p_{ch} is simply set to 0, and the coefficient $\mathscr{W}_{\mathrm{ch},2}$ equal to 1. The volume changes experienced during the experiments of Huang and Meek (1999) are quite large, so that a finite strain formulation is required.

The stromal specimens are in continuing equilibrium with a bath of controlled chemical composition and pressure. The simulations mimic the experiments and proceed in four stages, sketched in Fig. 12:

- In the initial state O, the bath has a hypertonic composition, with a concentration of sodium chloride equal to 1 mole per liter, a pH equal to 7, and, according to Table 3 of Huang and Meek (1999), hydration equal to 5.6.
- Stage OA: the ionic strength of NaCl in the bath is brought to 30 mM.

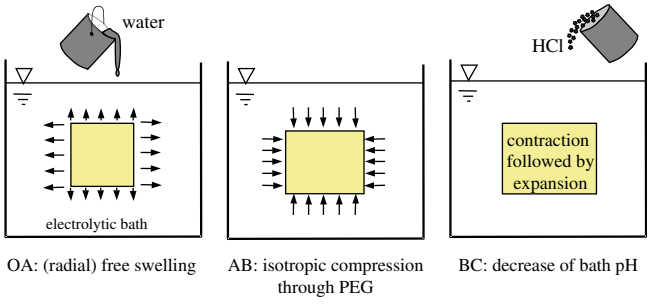

Fig. 12. Schematic of the three sequences of the chemo-mechanical tests on corneal stroma by Huang and Meek (1999). OA: free swelling starting from hypertonic state; AB: isotropic compression through PEG at fixed bath chemical composition; BC: decrease of bath pH.

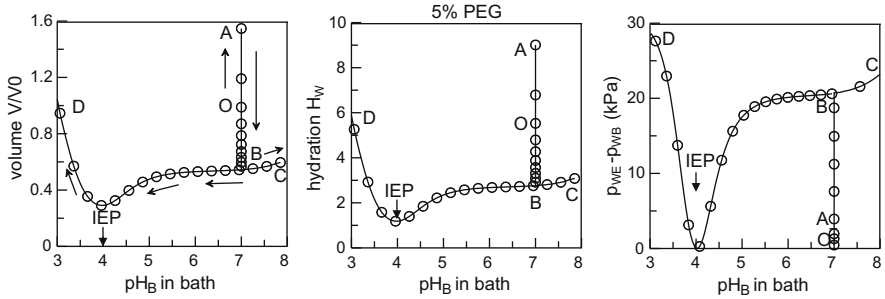

Fig. 13. Stroma in equilibrium with a bath of controlled chemical composition, and subjected to a mechanical load through polyethylene glycol PEG at 5%. Evolution of the volume, hydration and osmotic pressure during the three loading stages OA, AB, and BCD. These three mechanical properties show an extremum at the IEP, around 4.

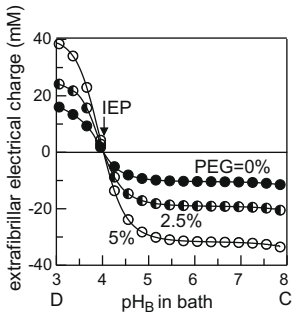

Fig. 14. Variation of the total extrafibrillar charge as a function of the pH of the bath, for the three loading tests through PEG.

- Stage AB: osmotic compression of the stromal specimens is realized through polyethylene glycol (PEG) whose concentration is brought to some target value, e.g. 5% of PEG corresponding to 27.75 kPa.
- Stage BCD: the pH of the bath is increased from 7 to 8, and next decreased from 8 to 3.

Osmotic compression is realized through various concentrations of polyethylene glycol (PEG) with molecular mass 20 kg. The pressure, measured in kPa, exerted by PEG can be estimated from the formula,

$$p_{\mathrm{PEG}} = 1.28 c_{\mathrm{PEG}} + 0.85 (c_{\mathrm{PEG}})^2, \tag{6.4}$$

the concentration c_{PEG} being measured in g of PEG per gram of solution multiplied by 100.

The isoelectric point, IEP about 4, is crossed in the third stage CD of the loading history. As indicated in Figs. 13 and 15, a number of entities show an extremum at the IEP, e.g. specimen volume, hydration, osmotic pressure. When no extra load is applied, the volumes in the hypertonic state and at the IEP are identical and minimal. When a compression is applied, the volume at the IEP is of course smaller than in the hypertonic state, point O, as illustrated in Fig. 13.

The profiles in terms of bath pH of the volume descriptors displayed in Figs. 13 and 15 and of the concentrations of ions and fixed charges are due to both a *chemo-mechanical coupling* and a *mechano-chemical coupling*. Indeed, since at the IEP, the electrical shielding vanishes, the volume is minimal, as indicated by the plots, and therefore some concentrations may increase, even if, at constant volume, they would decrease. The fact that the mechano-chemical coupling is strong may also be appreciated by considering the significant increase of the concentrations of ionic and fixed charges with the PEG loading, Fig. 14. The phenomenon is to be traced to the low radial moduli which allow both large volume increase and decrease.

Below the IEP, collagen becomes positively charged, while the charge of PG's fades out. Repulsion between close charges leads, through macroscopic electro-chemical coupling, to large osmotic pressures, and through chemo-mechanical coupling, to a large volume expansion along the radial direction.

Even if the experiments involve complex and severe chemical and mechanical loadings, and the mechanical model is rather crude, it is worth noting that the simulations match the data qualitatively and quantitatively well, as witnessed by Fig. 15.

7. Conclusions

The main issues addressed in this work can be listed as follows:

- A constitutive framework has been developed: it is consistent with the thermodynamics of porous media, including chemo-mechanical couplings in presence of several metallic

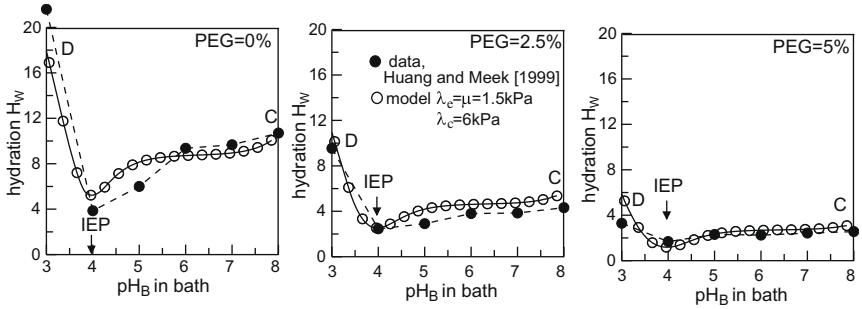

Fig. 15. Stroma in equilibrium with a bath of controlled chemical composition, and subjected to a mechanical load through polyethylene glycol PEG at 0%, 2.5% and 5%. Hydration as a function of bath pH during stage CD. The hydration is minimum at the IEP. In absence of compression, a large volume expansion takes place at low pH due to collagen becoming positively charged.

ions, hydrogen and hydroxyl ions, accounting for water dissociation, calcium binding for articular cartilages, chloride binding for corneal stroma, and resulting in chemo-hyperelastic constitutive equations.

- The fact that the collagen fibers are mechanically active only in extension results in a directional response, even if the spatial distribution of the fibers is random. In presence of chemically induced swelling, chemo-mechanical coupling results in stiffening of the mechanical response due to fiber recruitment. Chemical shrinking has opposite effects. The phenomenon is quantified through the angle β_m which is a measure of the size of the cones of fibers which are mechanically active.
- Progressive uncrimping of the fibers is not directly accounted for, but replaced by an overall nonlinear stress–strain law. For articular cartilages, the influence of this nonlinearity on the chemical variables is small. In fact, a model in which fibers have a linear mechanical behavior in extension, namely for small k_c in (4.3), yields virtually the same results for chemical variables (concentrations, etc.), but of course not for mechanical variables (stress, strain, etc.).
- The chemo-mechanical response accounts for both electric shielding at large ionic strength, and variation of the fixed electric charge (the key engine of electro-chemo-mechanical couplings) due to acid–base reactions, calcium or chloride binding.
- For both articular cartilages and corneal stroma, the chemo-mechanical coupling is strong: changes of the concentrations of ions and fixed charges imply significant changes in strains at given stresses, or in stresses at given strains. The converse mechano-chemical coupling is strong only in corneal stroma due to the large compliance of the matrix.

The simulations have assumed a random directional distribution of collagen fibrils. Still, the influence of a non-isotropic collagen network, displaying rotational symmetry about the traction axis has been tested for articular cartilages. The directional distribution $\Phi(\beta)$ is described by a single harmonic,

$$\Phi(\beta) = \frac{\Phi_0}{4\pi} + \frac{3}{4\pi}(1-\Phi_0)(\cos\beta)^2, \tag{7.1}$$

with a coefficient $\Phi_0 \in]0, 3/2[$. The ratio of the fiber density along the symmetry axis and in an orthogonal direction is equal to $3/\Phi_0 - 2$. Isotropy corresponds to $\Phi_0 = 1$. While the various mechanical entities depend strongly on the collagen directional distribution, the stress ratios displayed in Fig. 11 are found to be quite insensitive to even relatively large deviations with respect to an isotropic collagen network.

Here, as a trade off, the chemo-mechanical model has exploited the osmotic pressure. The key advantage is that arbitrary types of ions are accounted for in a straightforward manner that does not require the determination of parameters. While the model embeds the salient features of the experimental data, the drawback is certainly its lack of accuracy. Calibration of a more complete chemo-mechanical model where the weight of individual ions is accounted for requires data along several chemical and mechanical loading paths (Loret and Simões, 2005a,b). Experimental measurements of stresses and strains in the three directions of space would be most welcome, so as to assess the three dimensional validity of the constitutive equations.

Experiments involving changes in pH and controlling the mechanical conditions at the boundaries are necessarily complex. A particular difficulty consists in defining a trustful reference state that can be used to compare the effects of the subsequent mechanical and chemical loading processes. The hypertonic state with large sodium chloride concentration and neutral pH has been used to start the simulations. On the other hand, one might argue that the loading processes that the specimens of articular cartilages and corneal stromas have undergone are so severe that the initial state may have been wiped out. In any case, despite the complexity of these loading processes, the simulations reproduce quite well the available data, which exhibit strong instances of chemo-mechanical coupling, or mechano-chemical coupling, or both.

References

Akizuki, S., Mow, V.C., Muller, F., Pita, J.C., Howell, D.S., Manicourt, D.H., 1986. Tensile properties of human knee joint cartilage: I. Influence of ionic conditions, weight bearing and fibrillation on the tensile modulus. Journal of Orthopaedic Research 4, 379–392.

Athanasiou, K.A., Rosenwasser, M.P., Buckwalter, J.A., Malinin, T.I., Mow, V.C., 1991. Interspecies comparisons of in situ intrinsic mechanical properties of distal femoral cartilage. Journal of Orthopaedic Research 9 (3), 330–340.

Eisenberg, S.R., Grodzinsky, A.J., 1985. Swelling of articular cartilage and other connective tissues: electromechanical forces. Journal of Orthopaedic Research 3, 148–159.

Elliott, G.F., Hodson, S.A., 1998. Cornea, and the swelling of polyelectrolyte gels of biological interest. Reports Progress in Physiology 61, 1325–1365.

Federico, S., Grillo, A., La Rosa, G., Giaquinta, G., Herzog, W., 2005. A transversely isotropic, transversely homogeneous microstructural-statistical model of articular cartilage. Journal of Biomechanics 38, 2008–2018.

Frank, E.H., Grodzinsky, A.J., 1987a. Cartilage electromechanics – I. Electrokinetic transduction and the effects of electrolyte pH and ionic strength. Journal of Biomechanics 20 (6), 615–627.

Frank, E.H., Grodzinsky, A.J., 1987b. Cartilage electromechanics – II. A continuum model of cartilage electrokinetics and correlation with experiments. Journal of Biomechanics 20 (6), 629–639.

Frank, E.H., Grodzinsky, A.J., Phillips, S.L., Grimshaw, P.E., 1990. Physicochemical and bioelectrical determinants of cartilage material properties. Biomechanics of diarthrodial joints. In: Mow, V.C., Ratcliffe, A., Woo, S.L.-Y. (Eds.), vol. I, pp. 261–282.

Grodzinsky, A.J., Roth, V., Myers, E., Grossman, W.D., Mow, V.C., 1981. The significance of electromechanical and osmotic forces in the non-equilibrium swelling behavior of articular cartilage in tension. Journal of Biomechanical Engineering: Transactions of the ASME 103, 221–231.

Hodson, S., Kaila, D., Hammond, S., Rebello, G., Al-Omari, Y., 1992. Transient chloride binding as a contributory factor to the corneal stromal swelling in the ox. Journal of Physiology 450, 89–103.

Huang, Y., Meek, K.M., 1999. Swelling studies on the cornea and sclera: The effects of pH and ionic strength. Biophysical Journal 77, 1655–1665.

Li, S.-T., Katz, E.P., 1976. An electrostatic model for collagen fibrils. The interaction of reconstituted collagen with Ca^{2+}, Na^{+}, and Cl^{-}. Biopolymers 15, 1439–1460.

Loret, B., Simões, F.M.F., 2004. Articular cartilage with intra- and extrafibrillar waters. A chemo-mechanical model. Mechanics of Materials 36 (5–6), 515–541.

Loret, B., Simões, F.M.F., 2005a. Mechanical effects of ionic replacements in articular cartilage. Part I – the constitutive model. Biomechanics and Modeling in Mechanobiology 4 (2–3), 63–80.

Loret, B., Simões, F.M.F., 2005b. Mechanical effects of ionic replacements in articular cartilage. Part II – simulations of successive substitutions of NaCl and $CaCl_2$. Biomechanics and Modeling in Mechanobiology 4 (2–3), 81–99.

Loret, B., Simões, F.M.F., 2007. Articular cartilage with intra- and extra-fibrillar waters. Mass transfer and generalized diffusion. European Journal of Mechanics-A/Solids 26, 759–788.

Loret, B., Simões, F.M.F., 2010. Effects of pH on transport properties of articular cartilages. Biomechanics and Modeling in Mechanobiology 9, 45–63.

Muir, H., 1978. Proteoglycans of cartilage. Journal of Clinical Pathology Supplementary 31 (Roy. Coll. Path.) (12), 67–81.

Muir, H., 1983. Proteoglycans as organizers of the intercellular matrix. Biochemical Society Transactions 11, 613–622.

Pezowicz, C.A., Robertson, P.A., Broom, N.D., 2005. Intralamellar relationships within the collagenous architecture of the annulus fibrosus imaged in its fully hydrated state. Journal of Anatomy 207, 299–312.

Plaas, A.H., West, L.A., Thonar, E.J.A., Karcioglu, Z.A., Smith, C.J., Klintworth, G.K., Hascall, V.C., 2001. Altered fine structures of corneal and skeletal keratan sulfate and chondroitin/dermatan sulfate in macular corneal dystrophy. Journal of Biological Chemistry 276 (43), 39788–39796.

Sasaki, N., Odajima, S., 1996. Stress–strain curve and Young's modulus of a collagen molecule as determined by the X-ray diffraction technique. Journal of Biomechanics 29, 655–658.

Wachtel, E., Maroudas, A., 1998. The effects of pH and ionic strength on intrafibrillar hydration in articular cartilage. Biochimica et Biophysica Acta 1381, 37–48.